Irradiation effects on the structural and optical properties of single crystal β-Ga2O3

Liu, C.; Berencén, Y.; Yang, J.; Wei, Y.; Wang, M.; Yuan, Y.; Xu, C.; Xie, Y.; Li, X.; Zhou, S.;

Originally published:

August 2018

Semiconductor Science and Technology 33(2018)9, 095022

DOI: https://doi.org/10.1088/1361-6641/aad8d1

Irradiation effects on the structural and optical properties of single crystal β-Ga_2O_3

Chaoming Liu[1,2], Yonder Berencén[2], Jianqun Yang[1], Yidan Wei[1], Mao Wang[2,3], Ye Yuan[2,4], Chi Xu[2,3], Yufang Xie[2,3], Xingji Li[1], and Shengqiang Zhou[2]

[1] Harbin Institute of Technology, School of Materials Science and Engineering, 150001, Harbin, China
[2] Helmholtz-Zentrum Dresden-Rossendorf, Institute of Ion Beam Physics and Materials Research, D-01328, Dresden, Germany
[3] Technische Universität Dresden, D-01062, Dresden, Germany
[4] Physical Science and Engineering Division (PSE), King Abdullah University of Science and Technology (KAUST), Thuwal 23955-6900, Saudi Arabia

E-mail: lxj0218@hit.edu.cn

Received xxxxxx
Accepted for publication xxxxxx
Published xxxxxx

Abstract

In the present work, we report the 25 MeV oxygen irradiation effects in *n*-type single crystal *β*-Ga_2O_3 at different fluences. We demonstrate that the symmetric stretching modes and bending vibrations of GaO_4 and GaO_6 units are impaired upon increasing O irradiation fluence. Blue and green photoluminescence emission bands are found to be mainly associated with gallium-oxygen divacancies, gallium vacancies and oxygen interstitials. The increase of optically active centers at low fluence and the photoluminescence quenching at high fluence are ascribed to the reduction of carrier density and the production of non-radiative recombination centers, respectively. The results envisage the possibility of obtaining pre-designed spectral behaviors by varying the oxygen irradiation fluence.

Keywords: β-Ga_2O_3, ion irradiation, photoluminescence, radiation defect

1. Introduction

Gallium oxide (Ga_2O_3) is a wide band gap semiconductor and exists commonly in five polymorphs α (corundum), β (monoclinic), γ (defective spinel), δ (orthorhombic), and ε (orthorhombic). Monoclinic beta-phase gallium oxide (*β*-Ga_2O_3) has received extensive attention as a versatile transparent conducting oxide semiconductor because of its ultra-wide band gap (4.6~4.9 eV), excellent chemical and thermal stability [1, 2]. The optical properties of single-crystal *β*-Ga_2O_3 can vary depending on the preparation methods and dopants [3]. Due to its tunable optical properties, *β*-Ga_2O_3 has been used for a wide variety of applications, such as transparent conducting oxide in optoelectronics [4], solar blind photodetectors [5], and optical waveguides [6].

A potential application in radiation environment is also of interest due to the higher formation energy of vacancy defects in *β*-Ga_2O_3 (53.3 eV for Ga vacancy) compared to that of other wide-band gap materials (7.02 eV for Ga vacancy in GaN, 3.3 eV for Si vacancy in 3C-SiC) [7-9]. Considering the potential applications in space environment, *β*-Ga_2O_3 material and device will commonly be irradiated by several types of particles and rays. In the space environment, the main sources of radiation damage are electrons, protons and heavy ions with energy ranging from a few tens of keV to many GeV [10]. However, low and medium energy (keV to MeV) particles are still important in radiation damage production because high energy particles will be "slowed down" to lower energies by the shield [7, 11, 12]. Therefore, studying the radiation effect of particles in MeV range is particularly important for the

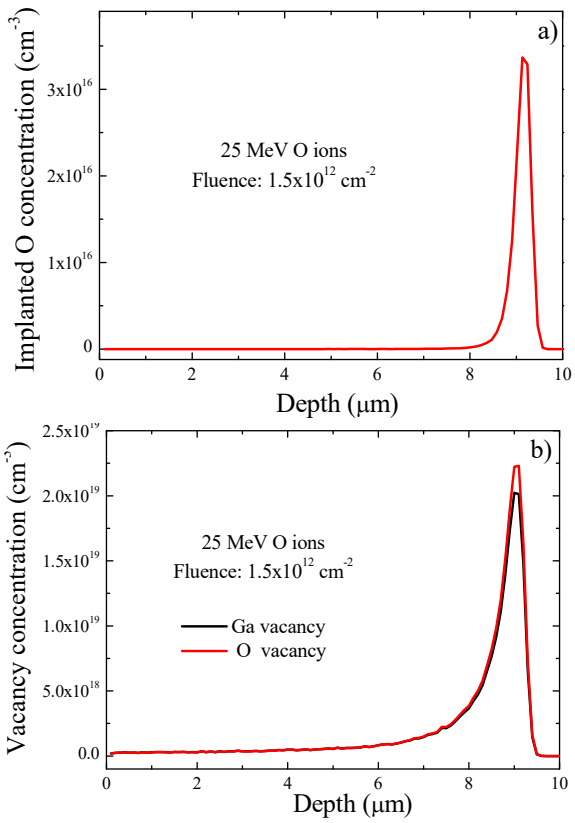

Fig. 1. Irradiation depth versus (a) implanted O concentration and (b) both O and Ga vacancy concentration in β-Ga_2O_3 with the O irradiation fluence of 1.5×10^{12} ions/cm^2.

actual effects simulation in space. Energetic particles lose their energy to ionizing (the production of electron-hole pairs) and non-ionizing processes (lattice displacement) as they travel through β-Ga_2O_3. The collision between an incoming ion and a lattice atom displaces the atom from its original lattice position, leading to vacancies, interstitials, and complexes of both [12, 13]. These defects will seriously influence the structural and optical properties of β-Ga_2O_3. However, to date limited information is available about the irradiation effects of β-Ga_2O_3 by gamma-rays [9], protons [7, 12] and electrons [13], and most focus on electrical characteristics. Further experimental investigation, particularly irradiation by heavy ions, is required for many applications of β-Ga_2O_3, since similar defects can be introduced during processing of β-Ga_2O_3 devices, e.g., ion-implantation doping as well as device operation exposed to a radiation environment.

Therefore, understanding the changes of the structural and optical properties of β-Ga_2O_3 caused by the ion radiation effects is of crucial importance. In this work, single crystal *n*-type β-Ga_2O_3 samples are irradiated by 25 MeV O ions with different fluences to investigate the irradiation effects on the structural and optical properties as well as the role of defects induced by radiation without introducing any other foreign element.

2. Experimental

A 600-μm-thick single crystal (-201) β-Ga_2O_3 wafer was purchased from MTI Corporation. The wafer was unintentionally doped with the Sn concentration of less than 1.0×10^{17} cm^{-3}. It was then cut into smaller pieces, which were subjected to room-temperature O ion irradiation at an energy of 25 MeV and different fluences at the Tandem Van de Graaff accelerator (Peking University, China). This procedure is expected to produce vacancies and interstitials without any other foreign element contamination at the same time. The charge state of O ions is +4, and an incident angle of 7° is applied to avoid the channeling effects. The irradiation fluences were chosen to be 1.5×10^{11} cm^{-2}, 5.0×10^{11} cm^{-2}, and 1.5×10^{12} cm^{-2}, respectively. The O ion flux was about 1.6×10^{8} atoms/cm^2 s.

To investigate the crystal structure of samples upon O irradiation, X-ray diffraction (XRD) was performed by a Bruker D8 advance diffractometer with a Cu-target source. The setup uses a Bragg-Brentano-geometry with a graphite secondary monochromator and a scintillator.

The monoclinic structure, stretching modes and bending vibrations of the samples were inspected by micro-Raman spectroscopy (Horiba-LabRAM) at room temperature. The Raman scattering was excited using a linearly polarized continuous 532 nm Nd:YAG laser with a liquid-nitrogen cooled CCD. In detail, the Raman spectra were recorded in backscattering geometry in the wavenumber range from 100 cm^{-1} to 900 cm^{-1} with a resolution of around 0.5 cm^{-1}.

The optical properties of the oxygen-irradiated β-Ga_2O_3 samples were investigated by room-temperature photoluminescence (PL) experiments using a 325 nm (~3.8 eV) He-Cd laser for the excitation with an optical power of about 35 mW, while a Xenon lamp coupled to a monochromator was used for the photoluminescence excitation (PLE) experiments. The emitted signal from the sample was collimated through a set of lenses and then dispersed by a Jobin Yvon Triax 550 monochromator to be ultimately recorded by a Si photodetector. A lock-in amplifier synchronized to an optical chopper at 20 Hz was used to enhance the signal-to-noise ratio.

3. Results and Discussion

Fig. 1 shows the simulation results of the O ion distribution and both O and Ga vacancies generated by each impinging O ion in β-Ga_2O_3 calculated by the SRIM code [14]. It can be observed that around 3.3×10^{16} oxygen/cm^3 can be injected into the β-Ga_2O_3 at the depth of about 9.5 μm when the O ion fluence is 1.5×10^{12} ions/cm^2. A maximum of the vacancy concentration induced by irradiation is observed at about 9 μm. The O vacancy concentration at the stopping

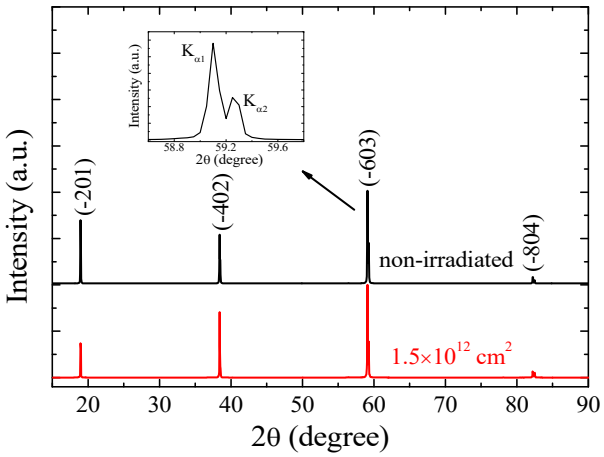

Fig. 2. XRD patterns of the irradiated and virgin β-Ga_2O_3 samples. The patterns were vertically shifted for better visibility.

region of O irradiation (~ 8.5-9.5 μm) is found to be higher than the Ga vacancy concentration. Note that the number of defects created by heavy ions are much more than the number of the implanted ions. The energy to create a vacancy-interstitial pair is in the range of 100 eV. According to SRIM simulation [14], each 25 MeV O ions can create around 2.84×10^7 vacancies (1.35×10^7 for V_{Ga} and 1.49×10^7 for V_O).

XRD analysis was performed to obtain the crystalline structure of the irradiated sample together with the non-irradiated sample, as shown in Fig. 2. As expected, the non-irradiated sample shows the diffraction peaks of β-Ga_2O_3 (-201), (-402), (-603) and (-804) planes. These diffraction peaks reveal a single crystal monoclinic β-Ga_2O_3 phase which is (-201) orientated. Peaks at higher angles 59.1° and 82.3°, show double lines corresponding to the $K_{\alpha1}$ and $K_{\alpha2}$ transitions. The peak at 59.0° is shown explicitly in the inset, where we observe a doublet peak with lesser intensity at 59.3° corresponding to the $K_{\alpha2}$ transition. For the irradiated sample with a fluence 1.5×10^{12} ions/cm^2, these four diffraction peaks still can be observed. The positions of diffraction peaks from XRD spectrum do not change upon irradiation significantly. However, the relative height of (-201) diffraction peak is decreased after irradiation. On the other hand, one would expect a lattice expansion along the perpendicular direction upon irradiation [15]. Such a measurement is beyond the detection resolution of the diffractometer used here.

β-Ga_2O_3 has a base-centered monoclinic structure with the space group symmetry of C_{2h}^3 (C2/m) [16]. The unit cell is composed of two types of gallium ions and three types of oxygen ions. According to the previous results [17], the irreducible representation for acoustical and optical modes is $\Gamma_{aco}=A_u+2B_u$ and $\Gamma_{opt}=10A_g+5B_g+4A_u+8B_u$, respectively. For the optical modes, A_g and B_g modes are Raman active, while A_u and B_u modes are infrared active. Fig. 3 shows the room-temperature micro-Raman spectra of the oxygen-irradiated β-Ga_2O_3 samples at different fluences together with a non-

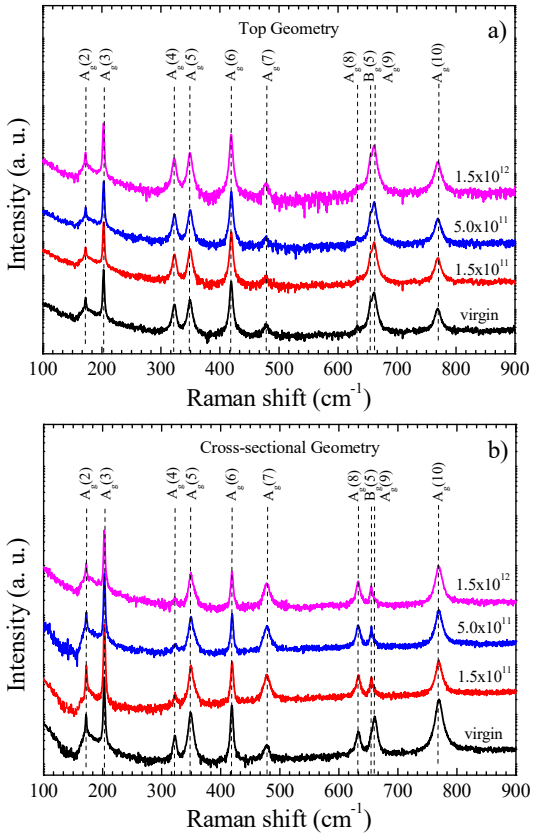

Fig. 3. Raman spectra of β-Ga_2O_3 samples at the top surface geometry (a) and the cross-sectional geometry (b). In the cross-sectional geometry, the excitation laser spot was focused around the depth of around 9 μm. One sees a clear decrease of the Raman intensity with increasing the irradiation fluence.

irradiated sample as a reference. It can be seen from the Fig. 3a) that all the A_g optical modes can be detected except the $A_g(1)$ mode at ~114 cm^{-1}, and $B_g(5)$ mode at 654cm^{-1} is observed, which is in good agreement with the results that have been reported [17-19].

According to the result published by Dohy *et al.* [17], Raman spectra of β-Ga_2O_3 samples can be classified into three groups, namely, A, B, and C to explore the phonon modes. For the group A (< 200 cm^{-1}), two low frequency modes peaking at 169 cm^{-1} ($A_g(2)$) and 200 cm^{-1} ($A_g(3)$) are found, which come from the vibration modes by liberation and translation of tetrahedra-octahedra chains in β-Ga_2O_3. Four main modes centered at 320 cm^{-1} ($A_g(4)$), 346 cm^{-1} ($A_g(5)$), 416 cm^{-1} ($A_g(6)$), and 475 cm^{-1} ($A_g(7)$) are observed in the group B (~310-480 cm^{-1}), which come from the GaO_2 octahedra symmetric stretching modes and the bending vibrations of GaO_6 units related to the optical modes. Three high frequency

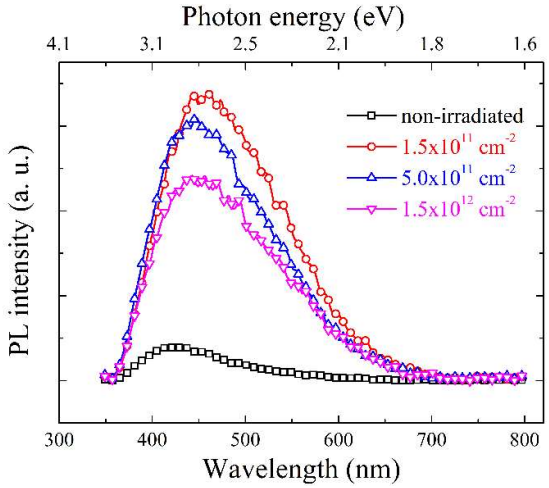

Fig. 4. Room-temperature PL spectra from the non-irradiated β-Ga_2O_3 and oxygen-irradiated samples at different fluences.

modes at 629 cm^{-1} ($A_g(8)$), 654 cm^{-1} ($B_g(5)$), 655 cm^{-1} ($A_g(9)$) and 766 cm^{-1} ($A_g(10)$) are originated by the GaO_4 tetrahedral bending and stretching related optical phonons in the group C (~500-770 cm^{-1}). However, compared with the non-irradiated sample, no noticeable change in these modes can be observed after O ion irradiation, as shown in Fig. 3a). The reason of this phenomenon could be that Raman spectra taken from the top surface ((-201) plane) cannot provide information from the region where defects are concentrated (the ion stopping region) in β-Ga_2O_3 due to the limited penetration depth of 532 nm laser.

To further investigate the effects in the defective region, Raman spectra were collected from the cross-section ((010) plane) of the β-Ga_2O_3 samples (as shown in Fig. 3b) and the laser spot (diameter: ~1μm) was fixed at around 9 μm from the surface using a high-precision translation stage. Compared with the results in Fig. 3a), there are no significant changes in the positions of the Raman modes recorded from cross-sectional geometry of β-Ga_2O_3. However, a remarkable change in the intensity of the Raman peaks compared to the non-irradiated sample is observed as the fluence increases. This behavior reflects the increasing disorder of the crystalline material with increasing fluence applied. From Fig. 3b), the modes in group A slightly change upon irradiation. The intensity of group B ($A_g(4)$, $A_g(5)$, $A_g(6)$) and group C ($A_g(9)$, $A_g(10)$) shows a visible decrease after O ion irradiation. These results indicate that O irradiation has no significant effect on the vibration modes by liberation and translation of tetrahedra-octahedra chains. Symmetric stretching modes and bending vibrations of GaO_6 and GaO_4 units are impaired upon the irradiation fluence. The decrease of the Raman intensity upon either ion implantation or irradiation has been observed in other semiconductors, such as GaN [20] and SiC [21].

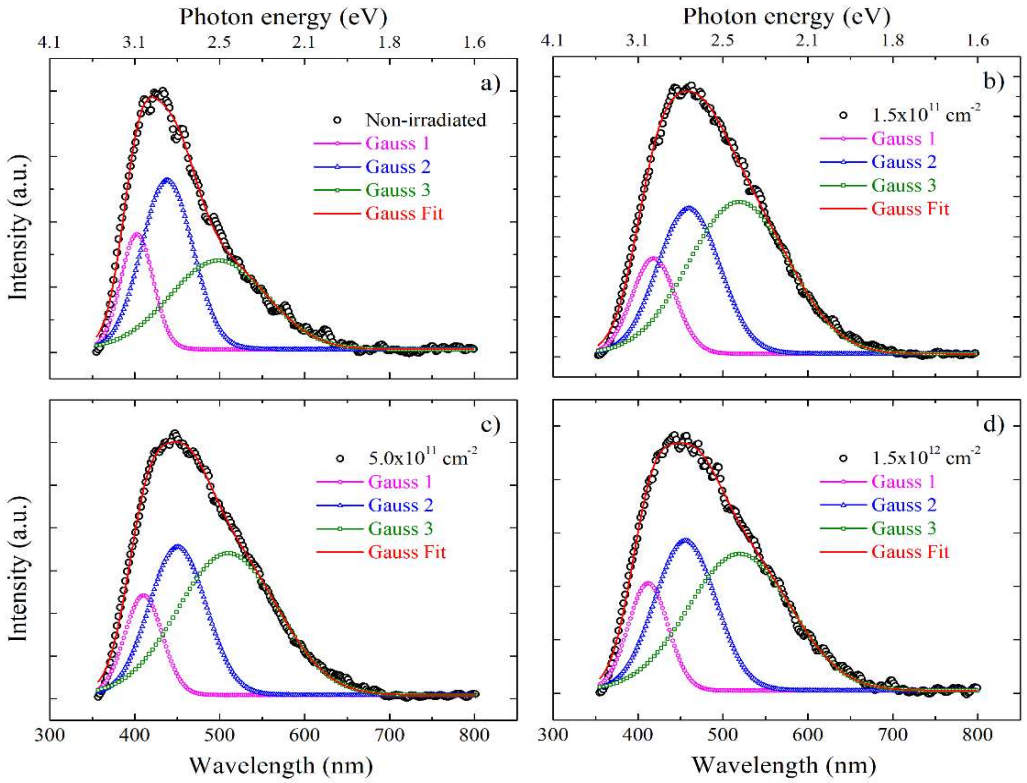

Fig. 5. Deconvoluted PL spectra by the Alentsev-Fock method of the non-irradiated β-Ga_2O_3 (a) and O-irradiated samples with the fluences of 1.5×10^{11} cm^{-2} (b), 5.0×10^{11} cm^{-2} (c) and 1.5×10^{12} cm^{-2} (d), respectively. Two blue PL bands and a green PL band can be resolved.

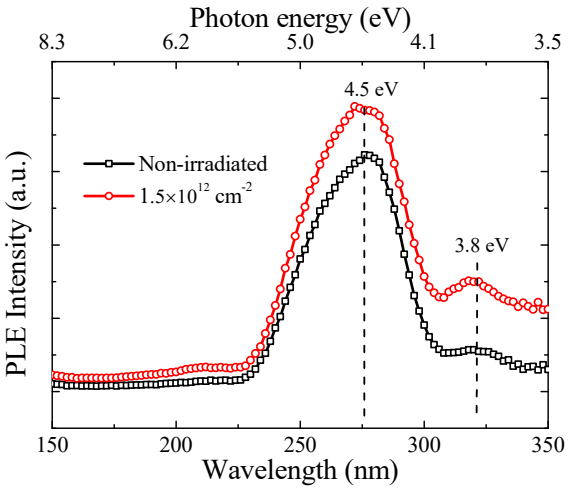

Fig. 6. Room-temperature PLE spectra of the non-irradiated β-Ga_2O_3 and the oxygen-irradiated sample.

The photoluminescence characteristic of β-Ga_2O_3 has been discussed in the past decades. β-Ga_2O_3 has been reported to exhibit a broad luminescence band composed of ultraviolet (UV), blue and green emission bands [22-24]. Room-temperature PL spectra of the β-Ga_2O_3 samples irradiated by O ions at different fluences are shown in Fig. 4. Each of the samples shows an asymmetric and broad PL band spanning from 350 nm to 800 nm. The intensity of the emission peak significantly increases upon O irradiation at low fluence as compared with the non-irradiated β-Ga_2O_3 sample. In addition, the luminescence intensity decreases as the O fluence increases, which indicates a quenching effect of PL intensity induced by O irradiation. The PL peak position has a red shift of about several tens of nanometers at the lower irradiation fluence. This red-shift is likely caused by the formation of new defect levels allowing for new optical transitions.

The PL spectra of the non-irradiated β-Ga_2O_3 and the oxygen-irradiated samples at different fluences were deconvoluted into two blue PL bands and a green PL band as shown in Fig. 5(a, b, c and d), respectively. The emission peak (λ_p), the energy (E), the full width at half maximum (FWHM), and the intensity (I), after applying the Alentsev-Fock method [25] are listed in Table 1. Fig. 5a) shows the deconvoluted PL luminescence spectra for the non-irradiated samples where three PL bands are found to be centered at around 402 nm (~3.08 eV), 438 nm (~2.83 eV) and 498 nm (~2.48 eV), respectively. Upon O irradiation, the position of these three peaks shifts around 20 nm to lower photon energies. By comparing the non-irradiated sample with the O-irradiated samples, an increase of the FWHM for the two blue PL bands is also observed, while the green PL band-related FWHM remains nearly without changes.

Table 1. PL emission bands after the spectral deconvolution of Fig. 5 using the Alentsev-Fock method. The peak position (λ_p), the corresponding energy (E), the FWHM and the intensity (I) are listed.

Sample	λ_p (nm)	E (eV)	FWHM (nm)	I (a.u.)
non-irradiated β-Ga_2O_3	402.69	3.08	45.03	3.52
	438.13	2.83	70.93	5.18
	498.54	2.48	134.06	2.71
1.5x10^{11} cm^{-2} O ions	418.43	2.96	60.06	23.82
	459.71	2.69	85.97	36.32
	519.15	2.38	138.83	37.91
5.0x10^{11} cm^{-2} O ions	414.41	2.99	52.15	23.32
	454.56	2.72	78.81	34.71
	516.05	2.40	138.93	33.21
1.5x10^{12} cm^{-2} O ions	412.95	3.00	55.22	20.07
	455.62	2.72	84.41	28.09
	519.61	2.38	142.51	25.59

In order to further investigate the band structure, PLE measurements were carried out at room temperature by monitoring the PL emission at 3.1 eV (400 nm) for the non-irradiated β-Ga_2O_3 and the oxygen-irradiated sample, as shown in Fig. 6. The room-temperature PLE spectra in both samples reveal two PLE bands for the 3.1 eV PL peak at 4.5 eV and 3.8 eV, respectively. The peak at 4.5 eV corresponds to the band gap, while the 3.8 eV PLE band is attributed to the recombination of conduction-band electrons with a self-trapped hole (STH) [26].

The different allowed optical transitions under sub-band gap PL excitation (3.8 eV) arising from intentionally *n*-type Si-doped β-Ga_2O_3 upon oxygen irradiation are schematically shown in Fig. 7. The origin of the three deconvoluted PL emission bands is thought to be related with the recombination of a bound exciton with the hole trapped at one of the different defects in β-Ga_2O_3. In detail, the blue band peaking at around 3.0 eV is ascribed to (V_{Ga} + V_O) divacancies in the (1-) charge state. The formation energy of this divacancy is reported to be lower than those of the isolated Ga vacancies (V_{Ga}) with (2-) and (1-) charge states, whereas the 2.7 eV blue PL emission correlates well with V_{Ga} with (2-) charge states [27]. Likewise, the 2.4 eV green PL emission is attributed to neutral oxygen interstitial (O_i^0) defects. Isolated V_{Ga}^{2-} (octahedral site) and V_{Ga}^{1-} (tetrahedral site) can also lead to green luminescence at 2.3 eV, but their corresponding formation energies are much higher than that of neutral O_i [27]. It is also worth mentioning that in our intentionally *n*-type Si-doped β-Ga_2O_3 samples, the Fermi level moves up leading to a stable charge state of V_{Ga}^{3-} defects in which the formation energy is much lower compared to that of (V_{Ga} + V_O)$^{1-}$ and O_i^0. This V_{Ga}^{3-}, however, can only result in a PL emission in the red-IR range [27].

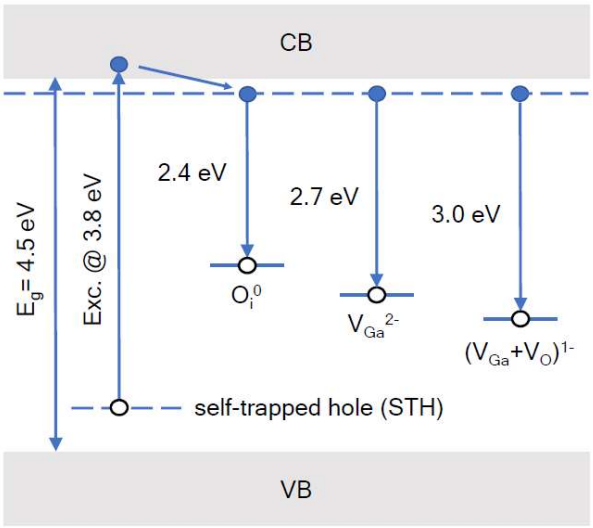

Fig. 7. Sketch of the band diagram with the different involved PL transitions of O-irradiated β-Ga_2O_3 samples under sub-band gap PL excitation

Two major effects of O irradiation on the PL properties can be distinguished: (i) the radiation induces an increase of PL intensity at low fluence and (ii) a quenching of the PL intensity at high fluence. Based on the above discussion, after O irradiation the concentration of the $(V_{Ga} + V_O)^{1-}$ divacancy and O interstitials increases resulting in the increase of the PL intensity. The PL quenching effect is most likely caused by the carrier density reduction and the production of non-radiative recombination centers by irradiation [28-30]. O irradiation strongly affects the lattice structure of gallium oxide and its periodic potential field, introducing the defect levels in the forbidden band. These defect levels produced by irradiation will reduce the carrier mobility in the material and creates deep-level centers which trap free carriers, resulting in the PL intensity quenching. Moreover, these deep level defects induced by O irradiation often act as non-radiative recombination centers and damp the luminescence efficiency [30], which thus lead to a decrease in PL intensity. The reduction of free carrier concentration by ion irradiation has also been observed in other wide bandgap semiconductors, such as GaN [31] and ZnO [32].

4. Conclusions

In conclusion, the effect of the oxygen irradiation on the structural and optical properties in *n*-type β-Ga_2O_3 single crystals has been investigated. We demonstrated that symmetric stretching Raman modes and bending vibrations of GaO_4 and GaO_6 units are impaired as the O irradiation fluence increases. Two blue luminescence bands at 3.0 eV and 2.7 eV have been found to be related to $(V_{Ga} + V_O)^{1-}$ divacancy and V_{Ga}^{2-} (octahedral site) defects respectively, and their corresponding intensities quench at the high O-irradiation fluences. An additional green PL band has been demonstrated to be originated from neutral O interstitials. These two blue- and the single green luminescence band intensities have been proven to increase at low O irradiation due to the increased optically active centers. However, at high fluence the increase of the deep level defect concentration via irradiation results in a reduction of the carrier density and the production of non-radiative recombination centers in β-Ga_2O_3. This leads to a decrease in the PL intensity at the investigated fluence range.

Acknowledgements

This work is supported by Science Challenge Project (No. TZ2018004), National Natural Science Foundation of China (No. 11775061 and No. 11205038) and the 111 Project under Grant No. B18017. The author C. L. (No. 201706125070) thanks financial support by Chinese Scholarship Council. The author Y. B. thanks the Alexander-von-Humboldt foundation for providing a postdoctoral fellowship. The support by Joerg Grenzer for XRD measurements is gratefully acknowledged.

Reference

[1] Pearton S J, Yang J, CaryIV P H, Ren F, Kim J, Tadjer M J and Mastro M A 2018 *Appl. Phys. Rev.* **5** 011301
[2] Ohira S, Suzuki N, Arai N, Tanaka M, Sugawara T, Nakajima K and Shishido T 2008 *Thin Solid Films* **516** 5763
[3] Fleischer M and Meixner H 1992 *J. Mater. Sci. Lett.* **11** 1728
[4] Ueda N, Hosono H, Waseda R and Kawazoe H 1997 *Appl. Phys. Lett.* **71** 933
[5] Zhang J, Li B, Xia C, Pei G, Deng Q, Yang Z, Xu W, Shi H, Wu F, Wu Y and Xu J 2006 *J. Phys. Chem. Solids* **67** 244
[6] Wang F, Han Z and Tong L 2005 *Physical E* **30** 150
[7] Yang G, Jang S, Ren F, Pearton S J and Kim J 2017 *ACS Appl. Mater. Interfaces* **9** 40471
[8] Wong M H, Sasaki K, Kuramata A, Yamakoshi S and Higashiwaki M 2016 *IEEE Electron Device Lett.* **37** 212
[9] Wong M H, Takeyama A, Makino T, Ohshima T, Sasaki K, Kuramata A, Yamakoshi S and Higashiwaki M 2018 *Appl. Phys. Lett.* **112** 023503
[10] Chenette D L, Chen J, Clayton E, Guzik T G, Wefel J P, Garcia-Munoz M, Lopate C, Pyle K R, Ray K P, Mullen E G, Hardy D A 1994 *IEEE T. Nucl. Sci.* **41** 2332
[11] Messenger S R, Xapsos M A, Burke E A, Walters R J and Summers G P 1997 *IEEE T. Nucl. Sci.* **44** 2169
[12] Ahn S, Lin Y H, Ren F, Oh S, Jung Y, Yang G, Kim J, Mastro M A, Hite J K, Eddy C R and Pearton S J 2016 *J. Vac. Sci. Technol.* B **34** 041213
[13] Yang J, Ren F, Pearton S J, Yang G, Kim J and Kuramata A 2017 *J. Vac. Sci. Technol.* B **35** 031208
[14] Ziegler J F, Ziegler M D and Biersack J P 2010 *Nucl. Instrum. Methods Phys. Res. Sect. B* **268** 1818
[15] Wang Y, Chen X, Li L, Shalimov A, Tong W, Prucnal S, Munnik F, Yang Z, Skorupa W, Helm M and Zhou S 2014 *J. Appl. Phys.* **115** 17C104
[16] Geller S 1960 *J. Chem. Phys.* **33** 676
[17] Dohy D, Lucazeau G and Revcolevschi A 1982 *J. Solid State Chem.* **45** 180

[18] Rao R, Rao A M, Xu B, Dong J, Sharma S and Sunkara M K 2005 *J. Appl. Phys.* **98** 094312
[19] Zhao Y and Frost R L 2008 *J. Raman Spectrosc.* **39** 1494
[20] Limmer W, Ritter W, Sauer R, Mensching B, Liu C and Rauschenbach B 1998 *Appl. Phys. Lett.* **72** 2589
[21] Li L, Prucnal S, Yao S D, Potzger K, Anwand W, Wagner A and Zhou S 2011 *Appl. Phys. Lett.* **98** 22
[22] López I, Nogales E, Méndez B, Piqueras J, Peche A, Ramírez-Castellanos J and González-Calbet J M 2013 *J. Phys. Chem. C* **117** 3036
[23] Onuma T, Fujioka S, Yamaguchi T, Higashiwaki M, Sasaki K, Masui T and T. Honda 2013 *Appl. Phys. Lett.* **103** 041910
[24] Mazeina L, Picard Y N, Maximenko S I, Perkins F K, Glaser E R, Twigg M E, Freitas J A and Prokes S M 2009 *Cryst. Growth Des.* **9** 4471
[25] Fok M V 1972 *Tr. FIAN* **59** 3
[26] Binet L and Gourier D 1998 *J. Phys. Chem. Solids* **59** 1241
[27] Ho Q D, Frauenheim T and Deák P 2018 *Phys. Rev. B* **97** 115163
[28] Pearton S J, Deist R, Ren F, Liu L, Polyakov A Y and Kim J 2013 *J. Vac. Sci. Technol. A* **31** 050801
[29] Buyanova I A, Wagner M, Chen W M, Monemar B, Lindström J L, Amano H and Akasaki I 1998 *Appl. Phys. Lett.* **73** 2968
[30] Pons D and Bourgoin J C 1985 *J. Phys. C: Solid State Phys.* **18** 3839
[31] Boudinov H, Kucheyev S O, Williams J S, Jagadish C and Li G 2001 *Appl. Phys. Lett.* **78** 943
[32] Kucheyev S O, Deenapanray P N K, Jagadish C, Williams J S, Yano M, Koike K, Sasa S, Inoue M and Ogata K I 2002 *Appl. Phys. Lett.* **81** 3350